



Optimization of radiation dosing schedules for proneural glioblastoma

H. Badri¹ · K. Pitter² · E. C. Holland³ ·
F. Michor^{4,5} · K. Leder¹

Received: 26 June 2014 / Revised: 4 June 2015 / Published online: 21 June 2015
© Springer-Verlag Berlin Heidelberg 2015

Abstract Glioblastomas are the most aggressive primary brain tumor. Despite treatment with surgery, radiation and chemotherapy, these tumors remain incurable and few significant increases in survival have been observed over the last half-century. We recently employed a combined theoretical and experimental approach to predict the effectiveness of radiation administration schedules, identifying two schedules that led to superior survival in a mouse model of the disease (Leder et al., *Cell* 156(3):603–616, 2014). Here we extended this approach to consider fractionated schedules to best minimize toxicity arising in early- and late-responding tissues. To this end, we decomposed the problem into two separate solvable optimization tasks: (i) optimization of the amount of radiation per dose, and (ii) optimization of the amount of time that

✉ K. Leder
lede0024@umn.edu

H. Badri
badri019@umn.edu

K. Pitter
kep2008@med.cornell.edu

E. C. Holland
eholland@fhcrc.org

F. Michor
michor@jimmy.harvard.edu

¹ Department of Industrial and Systems Engineering, University of Minnesota, Minneapolis, MN 55455, USA

² Weill Cornell Medical College, New York, NY 10065, USA

³ Division of Human Biology, Fred Hutchinson Cancer Research Center, Seattle, WA 98195, USA

⁴ Department of Computational Biology, Dana-Farber Cancer Institute, Boston, MA 02215, USA

⁵ Department of Biostatistics, Harvard T.H. Chan School of Public Health, Boston, MA 02115, USA

passes between radiation doses. To ensure clinical applicability, we then considered the impact of clinical operating hours by incorporating time constraints consistent with operational schedules of the radiology clinic. We found that there was no significant loss incurred by restricting dosage to an 8:00 a.m. to 5:00 p.m. window. Our flexible approach is also applicable to other tumor types treated with radiotherapy.

Keywords Brain tumors · Radiotherapy · Nonlinear programming · Linear-quadratic model

Mathematics Subject Classification 90C11 · 90C26 · 90C30 · 90C90 · 65K05

1 Introduction

Glioblastomas (GBMs) are the most frequent and malignant primary brain tumor, with an incidence of about 3.4 per 100,000 people in the US (Howlader et al. 2013). These tumors are aggressively treated with surgery, chemotherapy and radiation, but have remained incurable with little improvements in survival over the last 50 years. Recent molecular profiling efforts have elucidated that GBMs consist of at least 3 subgroups that are dominated by specific signaling pathways (Brennan et al. 2009; Phillips et al. 2006a, b; Verhaak et al. 2010). These subgroups include the proneural GBMs that are related to abnormal platelet-derived growth factor (PDGF) signaling, the classical GBMs that are driven by EGFR signaling, and the mesenchymal group that is associated with NF1 loss. The discovery of these subgroups has enabled the development of subtype specific mouse models to accurately mimic the different variants of GBM. We recently took advantage of one such model to revisit the question of optimum radiation administration in proneural GBMs (Leder et al. 2014).

Radiotherapy for glioblastoma is currently administered in 2Gy fractions five days a week, for 6 weeks total, as the clinical standard of care. Over the past thirty years there have been several clinical trials that have investigated the survival benefit of various fractionation schedules for glioblastoma. In particular, studies have investigated the benefits of hyper fractionated, hypo fractionated and accelerated fractionation schedules. Unfortunately none of these schedules has yet shown a significant survival benefit (Laperriere et al. 2002).

In our earlier work (Leder et al. 2014) we considered a dynamic radiation response model calibrated to a PDGF-driven glioma mouse model. Our model considered two separate populations of cells: stem-like glioma cells that are largely radio-resistant (Pajonk et al. 2010; Rich 2007) and differentiated glioma cells that are predominantly radiosensitive. The model stipulates that after exposure to radiation, a fraction of the differentiated cells can rapidly revert to the radio-resistant state (Bleau et al. 2009; Chen et al. 2012; Charles et al. 2010). We then used heuristic optimization techniques to find radiation delivery schedules that would lead to a significant model-predicted survival benefit over standard fractionation schedules. The increased efficacy of these schedules was then verified experimentally by survival studies in a mouse model of PDGF-driven glioma. In particular, 1-week optimized schedules predicted to outperform the standard schedule lead to a nearly 1.5-fold improvement in the median

survival time following irradiation, and had a similar overall survival compared to two weeks of standard therapy.

The building block for virtually all mathematical modeling of radiation response, including our previous work, is the linear-quadratic model (LQ), which matches well with experimental evidence across a wide range of clinically relevant radiation doses and fractionation schemes (Fowler 1989; Brenner 2008). The basic model states that following exposure to d Gy (SI derived unit of ionizing radiation), the reproductively viable fraction of cells is given by $e^{-\alpha d - \beta d^2}$. The two parameters α and β depend on the tissue type that is being irradiated. The parameter α represents killing of cells from a single track of radiation, and β represents the killing of a cell via two independent tracks of radiation (Hall and Giaccia 2006). There are several mathematical extensions to the LQ framework to incorporate additional biological phenomena such as repopulation of the tumor population between fractions, re-oxygenation of the tumor (this is required for some radiation therapy to be effective), the effectiveness of DNA repair mechanisms between fractions, and the redistribution of tumor cells within the cell cycle. Taken together these four extensions are often referred to as the '4Rs' and there have been several works based on these extensions (Withers 1975).

Many researchers have used modified versions of the LQ model to find clinically relevant optimal radiation delivery schedules. Previous reports have independently modeled the effect of either fixed or dynamic fractionation schemes (Brenner et al. 1998; Lu et al. 2008), the effect of incomplete DNA damage repair (Bertuzzi et al. 2013), the impact of the 4R's and tumor proliferation (Yang and Xing 2005), and the impact of hyper- or hypo-fractionated schedules (Unkelbach et al. 2013; Mizuta et al. 2012). Dionysiou et al. (2004) further examined hyper-fractionating using a novel four-dimensional simulation model of GBM and observed an increased tumor reduction when compared to standard fractionation. Subsequent work (Stamatikos et al. 2006) improved upon that simulation and found that an accelerated hyper-fractionated therapy has a good performance. The LQ framework has also been combined with models of glioma invasive growth patterns to predict the response to various radiation dose schedules and distributions (Harpold et al. 2007; Rockne et al. 2009).

As outlined above, there has been a significant amount of research dedicated to the subject of radiotherapy optimization. Some important questions in radiotherapy optimization concern the best total treatment size, the best way to divide the total dose into fractional doses, and the optimal inter-fraction interval times. An important constraint to enforce when answering these questions is sufficiently low levels of normal tissue toxicity. Thus a natural optimization problem will be to design a schedule that delivers radiation in such a way that does not exceed a given threshold level of normal tissue damage while achieving the maximal amount of tumor damage. In order to properly model normal tissue damage, we impose two simultaneous constraints: (i) the normal tissue with a relatively high turnover rate that reacts quickly to radiation (i.e. early-responding tissue, such as skin) does not experience excessive damage, and (ii) the slow-responding tissue with a relatively slow turnover rate (late-responding tissue, such as neurons) does not experience excessive damage. The two constraints are achieved by insisting that BED levels for the two tissues stay within prescribed

levels. Note that this problem is present in all uses of the standard BED model of tissue damage due to radiation.

Our prior results (Leder et al. 2014) demonstrated a proof of concept that radiation scheduling decisions have the potential to impact treatment efficacy. In order to further investigate this potential, we now construct a non-linear mathematical program to address the issue of normal brain toxicity, which was not addressed in our initial work. In our prior work it was observed that there was a leveling off of efficacy in the mouse model at 10 Gy, and we thus limited our study to treatments that considered 10 Gy total. Further we observed that this amount of radiation, in mice, elicits no dose-limiting toxicity even when administered all at once. However, in order to move the predictions of this model to a clinical trial with human patients, it is necessary to also ensure that any recommended schedule maintains a fixed level of normal tissue damage. Therefore, here we consider 10 Gy schedules and add constraints that specify that the radiation damage to normal tissue be within levels attained by a standard fractionation. The standard method for measuring tissue toxicity is done via the biologically equivalent dose (BED) (Fowler 1989, 2010). With these added constraints, the problem of finding the optimal radiation delivery schedule becomes quite difficult. Specifically, it involves finding optimal radiation doses at each fraction, time between fractions, and total number of fractions administered. To tackle this complex question, we decompose the optimization problem into two separate problems: (i) what is the optimal inter-fraction times, and (ii) what is the optimal radiation dose per fraction.

This work focuses on 10 Gy schedules, but we view it as an important step in the study of 60 Gy schedules used in the clinic. In particular, we believe that the methods we study here can be further developed to allow for the study and optimization of these larger schedules. These extensions are planned for future work.

In this paper, we will first review the mathematical model derived by Leder et al. (2014). We then formulate an optimization problem for the optimal radiation delivery schedule and present a solution to the optimization problem. Subsequently optimized schedules are found based on parameters from Leder et al. (2014). In addition we utilize simulated annealing to locate optimal inter-treatment times while observing standard working hour constraints. Finally we discuss the results and provide an outlook to future studies.

2 The mathematical model

Our model is based on a simplified version of the model studied by Leder et al. (2014). In the remainder of this subsection we will describe the model from the paper by Leder et al. (2014), and point out along the way the simplifying assumptions we make to develop the model for the current work.

Leder et al. (2014) studied response of a two cell type tumor model including stem-like glioma (radio-resistant) cells and differentiated glioma (radio-sensitive) cells to radiation. After exposure to radiation, a fraction of differentiated and stem-like tumor cells dies. This fraction is calculated using the LQ model. Of those differentiated cells that survive, a fraction γ (which depends on time since previous dose of radiation) dedifferentiate to a stem-like state at a rate ν . If it has been t_0 hours since the previous dose of radiation then we have

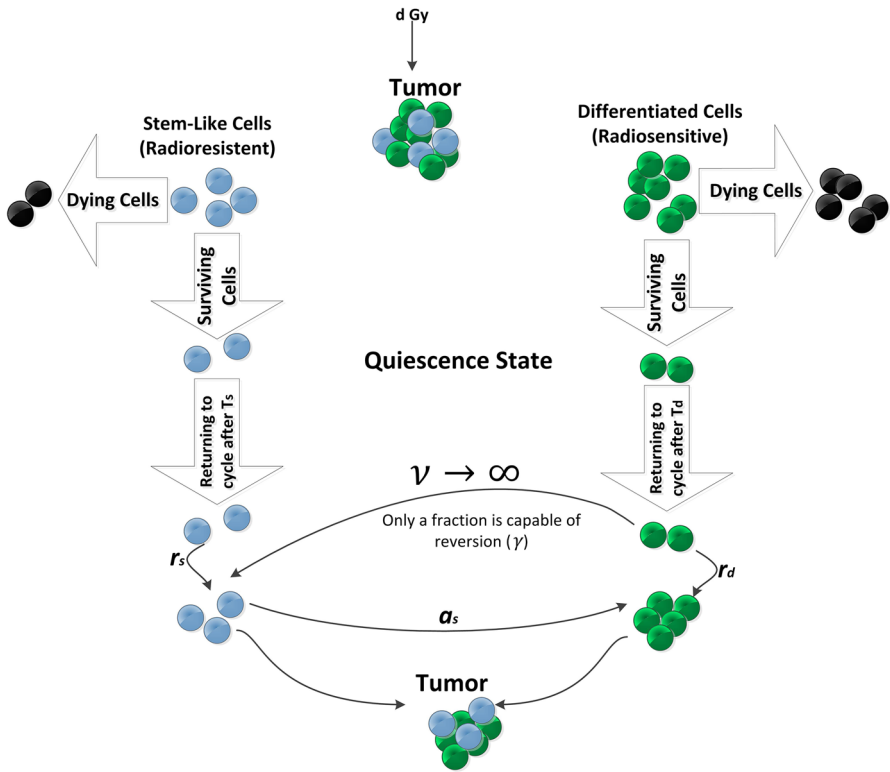


Fig. 1 Mathematical model description

$$\gamma(t_0) = \begin{cases} \gamma_0 \exp[-(t_0 - \mu)^2/\sigma^2], & t_0 < \infty \\ \gamma_0, & t_0 = \infty \end{cases}$$

where γ_0 , μ , and σ^2 are model parameters. The interpretation of $t_0 = \infty$ is that we are considering the effects of the first exposure to ionizing radiation. In particular, after the first dose of radiation a fraction γ_0 of cells is capable of dedifferentiation, the fraction capable of dedifferentiation after each subsequent dose depends on the time elapsed since the previous dose [as specified by the function $\gamma(t)$ for $t < \infty$].

Following exposure to ionizing radiation stem-like and differentiated cells stay, respectively, for T_s and T_d hours in a quiescent state and once they return to the cycle, they start to reproduce at a rate of r_s and r_d , respectively. Also stem-like cells produce differentiated cells at a rate of a_s . Figure 1 describes the mathematical model of glioma cell dynamics in response to radiation therapy.

It has been observed in several experimental settings that stem cells do in fact have a heightened radio resistance. Based on these observations in our previous work we assumed that radiation response of differentiated and stem-like cells were given by (α_d, β_d) and (α_s, β_s) with the simplifying assumption that $(\alpha_s, \beta_s) = \rho(\alpha_d, \beta_d)$ for some $\rho \in (0, 1]$. However in our previous work (Leder et al. 2014) we observed that

due to the slow growth kinetics of the stem-like cell population the parameter ρ has little impact on the system when considering disease dynamics over relatively short time intervals (approximately 6–12 weeks). Due to this phenomena discussed by Leder et al. (2014) we observed that it was still possible to match experimental data with $\rho = 1$, i.e., no added radio resistance in the stem-like cell population. It should be noted that when modeling human disease dynamics, where recurrence occurs over a much longer time scale, it is very possible that it is not appropriate to use $\rho = 1$. Since this work is focused on shorter time scales of both treatment and possible recurrence times we set $\rho = 1$, i.e., $(\alpha_s, \beta_s) = (\alpha_d, \beta_d) = (\alpha, \beta)$.

Based on the description given above we can specify a mathematical model for how the two tumor cell populations evolve as a function of time since exposure to radiation, time elapsed since previous exposure and amount of radiation given. Specifically, if we assume there are N^d and N^s differentiated and stem-like cells respectively at the time of exposure to d Gy of radiation, it has been t_0 hours since the previous exposure to radiation, then the population of differentiated and stem-like cells t hours after this exposure is given by

$$\begin{aligned}
 N^d(t, t_0) &= N^d e^{-\alpha d - \beta d^2} \left[(1 - \gamma(t_0)) e^{r_d(t - T_d)^+} + \gamma(t_0) e^{-\nu t} \right. \\
 &\quad \left. + a_s \gamma(t_0) \nu \int_0^t e^{r_d(t-s)} \int_0^{(s - T_s)^+} e^{-\nu y} e^{r_s(s-y - T_s)^+} dy ds \right] \\
 &\quad + a_s N^s e^{-\alpha d - \beta d^2} \int_{T_s}^{t \vee T_s} e^{r_s(s - T_s)} e^{r_d(t-s)^+} ds \\
 N^s(t, t_0) &= N^s e^{-\alpha d - \beta d^2} e^{r_s(t - T_s)^+} + \gamma(t_0) N^d e^{\alpha d - \beta d^2} \nu \int_0^t e^{-\nu s} e^{r_s(t-s - T_s)^+} ds.
 \end{aligned}$$

Since the mathematical model above is unwieldy and difficult to analyze, we will make some parameter assumptions to simplify the analysis. In particular, we first send $\nu \rightarrow \infty$, i.e., we assume that the dedifferentiation phenomena occurs immediately after radiation. In Lemma 3 we show that for $a > 0$ and any function f continuous at 0 we have

$$\lim_{\nu \rightarrow \infty} \nu \int_0^a e^{-\nu y} f(y) dy = f(0).$$

Which leads to the following

$$\begin{aligned}
 N^d(t, t_0) &= N^d e^{-\alpha d - \beta d^2} \left[(1 - \gamma(t_0)) e^{r_d(t - T_d)^+} \right. \\
 &\quad \left. + 1_{\{t > T_s\}} a_s \gamma(t_0) \int_{T_s}^t e^{r_d(t-s)} e^{r_s(s - T_s)} ds \right] \\
 &\quad + a_s N^s e^{-\alpha d - \beta d^2} \int_{T_s}^{t \vee T_s} e^{r_s(s - T_s)} e^{r_d(t-s)^+} ds \\
 N^s(t, t_0) &= N^s e^{-\alpha d - \beta d^2} e^{r_s(t - T_s)^+} + \gamma(t_0) N^d e^{-\alpha d - \beta d^2} e^{r_s(t - T_s)^+}.
 \end{aligned} \tag{1}$$

Table 1 Definition of model parameters used in our study

Parameter	Description
N_i^d and N_i^s	The population of differentiated and stem-like cells prior to treatment i , respectively
F_i^d and F_i^s	The fraction of differentiated and stem-like cells prior to treatment i , respectively
α and β	The parameters characterize the response of glioma cells to radiation
γ_i	The fraction of differentiated cells that revert to a stem-like state following treatment i
T_d	Time it takes for differentiated cell to return to cycle
T_s	Time it takes for stem-like cells to return to cycle
r_d	The rate at which differentiated cells reproduce once they return to cycle
r_s	The rate at which stem-like cells reproduce once they return to cycle
R	The initial ratio of differentiated cells to stem-like cells
a_s	The rate at which stem-like cells produce differentiated cells
T_p	Time it takes to complete the treatment for a patient (planning period)
T_e	Time after the conclusion of therapy when the performance of a schedule is evaluated
α_e and β_e	The parameters characterize the response of early responding normal tissues to radiation
α_l and β_l	The parameters characterize the response of late responding normal tissues to radiation
δ_e and δ_l	The proportional of radiation doses absorbed by early and late responding tissues, respectively
C_e and C_l	The maximum limit of BED for early and late responding normal tissues, respectively

The parameters used in our model are summarized in Table 1.

2.1 Decision variables and evolution during treatment

The primary goal of this paper is the mathematical optimization of radiotherapy fractionation schedules. In order to do this we need to now describe the available decision variables, and further how the tumor cell populations evolve during the course of multiple exposures to radiation. Our decision variables are inter-fraction times, fraction sizes, and number of fractions. Specifically we define t_i as the intermediate time between treatment i and $i + 1$, d_i the size of dose given in the i th fraction (Gy) and N the total number of fractions delivered.

In order to describe the population evolution, we first define the population at the epochs of fraction delivery. We denote the population of the differentiated and stem-like cells immediately prior to fraction i by N_i^d and N_i^s respectively. In addition, we will work with fraction of initial populations throughout this paper, i.e., $F_i^d = \frac{N_i^d}{N_1^d}$ and $F_i^s = \frac{N_i^s}{N_1^s}$. Lastly, we add the inter fraction times to the function $\gamma(\cdot)$,

$$\gamma_i = \begin{cases} \gamma_0 \times e^{-\frac{(t_{i-1}-\mu)^2}{\sigma^2}}, & i \geq 2 \\ \gamma_0, & i = 1. \end{cases}$$

It is possible to substantially simplify (1) in the setting of tumor population evolution between radiation fraction deliveries. This is achieved by assuming that the inter fraction times are always less than T_s . If we know the fraction of differentiated cells, F_i^d , immediately prior to treatment i and we administer d_i Gy in treatment i then

$$F_{i+1}^d = F_i^d (1 - \gamma_i) e^{r_d(t_i - T_d)^+} e^{-\alpha d_i - \beta d_i^2}, \quad i = 1, \dots, N - 1.$$

If we further assume that the inter fraction times are less than T_d then we have that

$$F_{i+1}^d = F_i^d (1 - \gamma_i) e^{-\alpha d_i - \beta d_i^2}, \quad i = 1, \dots, N - 1. \quad (2)$$

Since we start the treatment with $F_1^d = 1$, we have

$$F_N^d = e^{-\sum_{i=1}^{N-1} (\alpha d_i + \beta d_i^2)} \prod_{i=1}^{N-1} (1 - \gamma_i) \quad (3)$$

We can perform a similar simplification for the evolution of the stem-like cells between fraction. Specifically if the fraction of differentiated and stem-like cells immediately prior to treatment i are F_i^d and F_i^s respectively and d_i Gy of radiation are administered in this fraction then

$$F_{i+1}^s = e^{-\alpha d_i - \beta d_i^2} F_i^s + R e^{-\alpha d_i - \beta d_i^2} \gamma_i F_i^d, \quad i = 1 \dots N - 1, \quad (4)$$

where $R = N_1^d / N_1^s$.

We will denote the tumor populations t hours after the conclusion of N fractions of radiation by $(N_N^d(t), N_N^s(t))$. These variables are evaluated using (1), of course after normalizing by the initial tumor populations we get formulas for $(F_N^d(t), F_N^s(t))$.

3 Mathematical optimization

In this section, we define the objective function of our problem. Then we formulate the radiation therapy scheduling problem as a non-linear mathematical model. Lastly the structure of the optimal policies are described.

3.1 Objective function

The performance of a schedule is evaluated by the fraction of original cells that are present T_e hours after the conclusion of a fractionated radiotherapy treatment. Thus the objective function of a schedule with N fractions is given by:

$$\frac{N_N^d(T_e) + N_N^s(T_e)}{N_1^d + N_1^s} = \frac{F_N^d(T_e) \times N_1^d + F_N^s(T_e) \times \frac{N_1^d}{R}}{N_1^d + \frac{N_1^d}{R}} = \frac{RF_N^d(T_e) + F_N^s(T_e)}{R + 1}$$

Note that if we are interested in minimizing the expression in the previous display, it of course suffices to minimize $RF_N^d(T_e) + F_N^s(T_e)$.

All considered fractionation schedules last the same number of hours, denoted by T_p . In addition, as mentioned in the introduction the focus of this work is on shorter length schedules and we therefore assume throughout the remainder of the work that $T_p < \min(T_s, T_d)$.

3.2 Problem formulation

We now consider the problem of finding fractionation schedules that lead to minimal population size while maintaining acceptable levels of normal tissue damage. Specifically we consider the problem

$$\text{Minimize}_{d_i, t_i, N} F_N^s(T_e) + RF_N^d(T_e) \tag{5}$$

Subject to:

$$\begin{aligned} \sum_{i=1}^{N-1} t_i &= T_p \\ \sum_{i=1}^N \left(\delta_l d_i + \frac{\beta_l}{\alpha_l} \delta_l^2 d_i^2 \right) &\leq C_l \\ \sum_{i=1}^N \left(\delta_e d_i + \frac{\beta_e}{\alpha_e} \delta_e^2 d_i^2 \right) &\leq C_e \\ d_i &\geq \delta \quad \forall i \\ t_i &\geq \epsilon \quad \forall i \end{aligned}$$

where the formulas relating $(F_N^d(T_e), F_N^s(T_e))$ to (F_N^d, F_N^s) , i.e., the relationship between the tumor cell populations T_e hours after the final fraction and the tumor cell population immediately prior to the final fraction are given by

$$F_N^d(T_e) = [c_2(1 - \gamma_N) + c_3\gamma_N]e^{-\alpha d_N - \beta d_N^2} F_N^d + c_4e^{-\alpha d_N - \beta d_N^2} F_N^s$$

and

$$F_N^s(T_e) = c_5e^{-\alpha d_N - \beta d_N^2} F_N^s + c_6\gamma_N e^{-\alpha d_N - \beta d_N^2} F_N^d.$$

The constants $c_i, i = 2, \dots, 6$ are given by

$$\begin{aligned}
c_2 &= e^{r_d(T_e - T_d)} \\
c_3 &= a_s \int_{T_s}^{T_e} e^{r_d(T_e - s) + r_s(s - T_s)} ds = \frac{a_s}{r_s - r_d} \left[e^{r_s(T_e - T_s)} - e^{r_d(T_e - T_s)} \right] \\
c_4 &= \frac{a_s}{R} \int_{T_s}^{T_e} e^{r_d(T_e - s) + r_s(s - T_s)} ds = \frac{a_s}{R(r_s - r_d)} \left[e^{r_s(T_e - T_s)} - e^{r_d(T_e - T_s)} \right] \\
c_5 &= e^{r_s(T_e - T_s)} \\
c_6 &= R e^{r_s(T_e - T_s)},
\end{aligned}$$

and are derived using (1).

We use the first constraint to ensure that all fractionation schedules last for the same length of time. The second and third constraints are BED limits for late and early responding normal tissues, respectively. The terms (α_e, β_e) and (α_l, β_l) characterize respectively the linear-quadratic response of early and late responding normal tissue to ionizing radiation. The terms δ_e and δ_l are the sparing factors of the early and late tissue that represent how much of the radiation dose these normal tissues receive. Since for the late responding tissues, no allowance of repopulation should normally be necessary, we can use the linear quadratic model to formulate their BED (Hall and Giaccia 2006). However for early responding tissues, we cannot simply use the linear quadratic model. One method of modeling BED for early responding tissue is to use a repopulation correction factor which depends on the tissue doubling time and the treatment duration (Dale and Jones 2007). Specifically, we use the Fowler (2010) formulation to model the BED of early responding tissues as

$$BED = \sum_{i=1}^N \left(\delta_e d_i + \frac{\beta_e}{\alpha_e} \delta_e^2 d_i^2 \right) - \frac{0.693}{\alpha_e T_{eff}} (T_p - T_k)^+ \quad (6)$$

where T_{eff} and T_k are time parameters defined as effective cellular doubling time and kick-off time, respectively. All parameters in $\frac{0.693}{\alpha_e T_{eff}} (T_p - T_k)$ are constants in our model, hence we can always assume this term as a constant and move it to the right hand side of the third constraint. Thus we can view C_l as the amount of BED incurred by late responding tissues from the standard fractionation, and C_e as the amount of BED incurred by early responding tissues from the standard fractionation after accounting for the repopulation correction in (6).

Since we are optimizing the number of fractions (N) and dose per fraction (d_i , $i = 1, \dots, N$) simultaneously, we cannot assign 0 Gy of radiation to any fractions (if one of the d_i becomes 0, we actually have $N - 1$ fractions). Also due to treatment cost such as running cost, human resource cost and etc., it is uneconomical to deliver very small dosages in treatment sessions. In order to address these issues we add the fourth constraint. Finally, the last constraint indicates that two consecutive fractions cannot be scheduled at the same time or immediately one after another (due to the same reasoning we used for $d_i \neq 0$).

In order to solve the optimization problem formulated in (5) it is necessary to express the objective in terms of our decision variables. To address this issue we establish the following result

Theorem 1 For any N ,

$$F_N^s + RF_N^d = (1 + R)e^{-\sum_{i=1}^{N-1}(\alpha d_i + \beta d_i^2)}.$$

Proof We will use induction to prove above theorem. First, it is obvious that above relationship holds when $N = 2$, now suppose it holds for $N - 1$ too, which means

$$F_{N-1}^s + RF_{N-1}^d = (1 + R)e^{-\sum_{i=1}^{N-2}(\alpha d_i + \beta d_i^2)}$$

Then $F_N^s + RF_N^d$ can be calculated by (2) and (4):

$$\begin{aligned} F_N^s + RF_N^d &= e^{-\alpha d_{N-1} - \beta d_{N-1}^2} F_{N-1}^s + R\gamma_0 e^{-\alpha d_{N-1} - \beta d_{N-1}^2} e^{-(t_{N-2} - \mu)^2 / \sigma^2} F_{N-1}^d \\ &\quad + RF_{N-1}^d (1 - \gamma_0 e^{-(t_{N-2} - \mu)^2 / \sigma^2}) e^{-\alpha d_{N-1} - \beta d_{N-1}^2} \\ &= e^{-\alpha d_{N-1} - \beta d_{N-1}^2} (F_{N-1}^s + RF_{N-1}^d) \\ &= (1 + R)e^{-\sum_{i=1}^{N-1}(\alpha d_i + \beta d_i^2)} \end{aligned}$$

Thus establishing the result. □

With this result we can replace F_N^s by $(1 + R)e^{-\sum_{i=1}^{N-1}(\alpha d_i + \beta d_i^2)} - RF_N^d$. Furthermore the first two constraints can be placed into the objective function:

$$\begin{aligned} \text{Minimize}_{d_i, t_i, N} & (Rc_4 + c_5)(1 + R)e^{-\sum_{i=1}^N(\alpha d_i + \beta d_i^2)} + [-R(c_5 + Rc_4 - c_2) \\ & + (c_6 - Rc_2 + Rc_3)\gamma_0 e^{-(t_{N-1} - \mu)^2 / \sigma^2}] e^{-\alpha d_N - \beta d_N^2} F_N^d. \end{aligned}$$

By replacing F_N^d with its value from (3), we get:

$$\begin{aligned} \text{Minimize}_{d_i, t_i, N} & e^{-\sum_{i=1}^N(\alpha d_i + \beta d_i^2)} \left\{ (Rc_4 + c_5)(1 + R) \right. \\ & \left. + [-R(c_5 + Rc_4 - c_2) + (c_6 - Rc_2 + Rc_3)\gamma_0 e^{-(t_{N-1} - \mu)^2 / \sigma^2}] \right. \\ & \left. \times \left[(1 - \gamma_0) \prod_{i=1}^{N-2} \left(1 - \gamma_0 e^{-(t_i - \mu)^2 / \sigma^2} \right) \right] \right\}. \end{aligned}$$

Finally by minimizing the natural logarithm of the objective function we get:

$$\begin{aligned}
 \text{Minimize}_{d_i, t_i, N} & - \sum_{i=1}^N (\alpha d_i + \beta d_i^2) + \ln \left\{ (Rc_4 + c_5)(1 + R) \right. \\
 & + \left[-R(c_5 + Rc_4 - c_2) + (c_6 - Rc_2 + Rc_3)\gamma_0 e^{-(t_{N-1} - \mu)^2 / \sigma^2} \right] \\
 & \left. \times \left[(1 - \gamma_0) \prod_{i=1}^{N-2} \left(1 - \gamma_0 e^{-(t_i - \mu)^2 / \sigma^2} \right) \right] \right\} \tag{7}
 \end{aligned}$$

Subject to:

$$\begin{aligned}
 \sum_{i=1}^{N-1} t_i &= T_p \\
 \sum_{i=1}^N \left(\delta_e d_i + \frac{\beta_e}{\alpha_e} \delta_e^2 d_i^2 \right) &\leq C_l \\
 \sum_{i=1}^N \left(\delta_l d_i + \frac{\beta_l}{\alpha_l} \delta_l^2 d_i^2 \right) &\leq C_e \\
 d_i &\geq \delta \quad \forall i \\
 t_i &\geq \epsilon \quad \forall i.
 \end{aligned}$$

3.3 Solution approach

We start by fixing the number of fractions N , i.e., we assume it is a constant. Then note that in the optimization problem in (7), we can divide the objective function in two parts. The first term only includes $\{d_i\}$ and the second term only contains $\{t_i\}$. In addition the constraints can be split in two sets as well. The first and last constraint only depend on the inter fraction times $\{t_i\}$ and the remainder only depend on $\{d_i\}$. Therefore for a fixed value of N , instead of solving (7), we can solve two independent models, given in (8) and (17). For the first model (8), we have a quadratic objective function constrained to two quadratic and N linear constraints where the decision variables are simply d_i . Also for the second model (17), we have a log function of t_i as the objective function constrained to N linear constraints with t_i as decision variables. Therefore instead of solving (7), we can solve two independent models for a fixed value of N and then find the optimal number of fractions (N) via a simple search algorithm.

Note that the following formulations are obtained by making several important assumptions. First, we assume dedifferentiation phenomena occurs immediately after radiation. Second, we consider the same radio-sensitivity parameters in both differentiated and stem-like cells, i.e. we assume there is no added radio resistance in the stem-like cell population. Third, since the focus of this paper is on shorter length schedules, we assume that treatment duration is shorter than the time to return to cycle of both the differentiated and stem cells. Lastly, we fix the the duration of all fractionation schedules to be T_p .

3.3.1 Model I

We can define the first model as the optimization model of radiation doses under the constraint of the radiation effect on normal tissues regardless of t_i as (8).

$$\text{Maximize}_{d_i} \sum_{i=1}^N (\alpha d_i + \beta d_i^2) \tag{8}$$

Subject to:

$$\begin{aligned} \sum_{i=1}^N \left(\delta_e d_i + \frac{\beta_e}{\alpha_e} \delta_e^2 d_i^2 \right) &\leq C_e \\ \sum_{i=1}^N \left(\delta_l d_i + \frac{\beta_l}{\alpha_l} \delta_l^2 d_i^2 \right) &\leq C_l \\ d_i &\geq \delta \quad \forall i \end{aligned}$$

Here, we are interested in finding the scheduled break-up of a radiotherapy treatment into a set of treatment increments in a way that complications in normal tissues remain within their acceptable limits. BED constraints can be transformed to the following forms:

$$\sum_{i=1}^N \left(d_i + \frac{1}{2} \frac{\alpha_e}{\beta_e \delta_e} \right)^2 \leq \frac{\alpha_e C_e}{\beta_e \delta_e^2} + N \left(\frac{1}{2} \frac{\alpha_e}{\beta_e \delta_e} \right)^2 \tag{9}$$

$$\sum_{i=1}^N \left(d_i + \frac{1}{2} \frac{\alpha_l}{\beta_l \delta_l} \right)^2 \leq \frac{\alpha_l C_l}{\beta_l \delta_l^2} + N \left(\frac{1}{2} \frac{\alpha_l}{\beta_l \delta_l} \right)^2 \tag{10}$$

The set of fractionated doses (d_1, \dots, d_N) satisfying (9) and (10) is represented by two N -dimensional hyperspheres (HSE) and (HSL), respectively. We can argue that the optimal solution lies on the feasible boundaries of (9) and (10). Since α and β are positive values, the objective function in (8) is always increasing in d_i . Assume (d_1^*, \dots, d_N^*) is optimal solution to (8) and it lies in the interior of the (9) and (10). If we increase one arbitrary element of d_i^* , we can keep the solution feasible and increase the objective function. Therefore it is not an optimal solution to our problem and the optima must lie on the most confining constraint, the constraint that imposes the largest restriction on the dose that can be delivered to the tumor [either (9) or (10)].

If we ignore the second constraint in (8) and only consider the BED limit for early responding tissues, we can find the limit of $\sum_{i=1}^N d_i^2$ from the first constraint as

$$\sum_{i=1}^N d_i^2 \leq \frac{C_e - \delta_e \sum_{i=1}^N d_i}{\frac{\beta_e}{\alpha_e} \delta_e^2}$$

Since β is a positive value, we see that:

$$\sum_{i=1}^N \alpha d_i + \beta d_i^2 \leq \sum_{i=1}^N \alpha d_i + \beta \frac{C_e - \delta_e \sum_{i=1}^N d_i}{\frac{\beta_e}{\alpha_e} \delta_e^2}$$

If we maximize the upper bound of the above equation, we can find the optimal answer to (8) while only considering one constraint. The upper bound optimization problem can be defined as:

$$\text{Maximize}_{d_i} \sum_{i=1}^N \alpha d_i + \beta \frac{C_e - \delta_e \sum_{i=1}^N d_i}{\frac{\beta_e}{\alpha_e} \delta_e^2}$$

Subject to:

$$\sum_{i=1}^N \left(\delta_e d_i + \frac{\beta_e}{\alpha_e} \delta_e^2 d_i^2 \right) = C_e$$

$$d_i \geq \delta \quad \forall i$$

By rearranging objective function, we can simplify it as:

$$\text{Maximize}_{d_i} \left(\alpha - \frac{\beta \alpha_e}{\beta_e \delta_e} \right) \sum_{i=1}^N d_i + \beta \frac{\alpha_e C_e}{\beta_e \delta_e^2} \tag{11}$$

The objective function can be interpreted as follows:

- (a) If $\alpha - \frac{\beta \alpha_e}{\beta_e \delta_e} > 0$, the larger $\sum_{i=1}^N d_i$ while restricted to the surface of the hypersphere is, the larger the damage effect on tumor is.
- (b) If $\alpha - \frac{\beta \alpha_e}{\beta_e \delta_e} < 0$, the smaller $\sum_{i=1}^N d_i$ while restricted to the surface of the hypersphere is, the larger the damage effect on tumor is.

Note that when $\alpha - \frac{\beta \alpha_e}{\beta_e \delta_e} = 0$, any point of the early constraint boundary is optimal. If we repeat the above steps when only considering the second constraint (late responding tissues), we will get:

$$\text{Maximize}_{d_i} \left(\alpha - \frac{\beta \alpha_l}{\beta_l \delta_l} \right) \sum_{i=1}^N d_i + \beta \frac{\alpha_l C_l}{\beta_l \delta_l^2}$$

Subject to:

$$\sum_{i=1}^N \left(\delta_l d_i + \frac{\beta_l}{\alpha_l} \delta_l^2 d_i^2 \right) = C_l$$

$$d_i \geq \delta \quad \forall i$$

The objective function can be interpreted as above in (a) and (b) with respect to the sign of the $\alpha - \frac{\beta\alpha_i}{\beta_i\delta_i}$. Therefore optimal schedule can be found by minimizing and maximizing $\sum_{i=1}^N d_i$ on the feasible boundaries (9) and (10). We first need the following technical lemma.

Lemma 1 *The set of $d_1 = \dots = d_N = \sqrt{\frac{C}{N}} + a$ and $d_1 = \dots = d_{N-1} = \delta, d_N = \sqrt{C - (N - 1)(\delta - a)^2} + a$ are maximizer and minimizer of $\sum_{i=1}^N d_i$ under two constraints as $\sum_{i=1}^N (d_i - a)^2 = C$ and $d_i \geq \delta$, respectively (C and δ are positive numbers).*

Proof The feasible region for the above model is compact and the objective function is continuous on it. It is obvious from the Weierstrass theorem that optima exist (Pierre 1969). We can use the KKT conditions (Pierre 1969) to find the necessary conditions for optima. We write down the KKT conditions (Pierre 1969) for the maximization problem first. In particular we have the following Lagrangian:

$$L = - \sum_{i=1}^N d_i + \nu \left[\sum_{i=1}^N (d_i - a)^2 - C \right] + \sum_{i=1}^N \lambda_i (d_i - \delta)$$

The next step is constructing KKT conditions:

$$\begin{aligned} \frac{\partial L}{\partial d_i} &= -1 + 2\nu(d_i - a) + \lambda_i = 0, \quad i = 1, \dots, N \\ \lambda_i (d_i - \delta) &= 0, \quad i = 1, \dots, N \\ \sum_{i=1}^N (d_i - a)^2 &= C \\ \nu &= \text{free}, \quad \lambda_i \leq 0, \quad i = 1, \dots, N \end{aligned}$$

From the second condition, either $\lambda_i = 0$ or $d_i = \delta$. Without loss of generality we assume that there is an integer m such that for $i = 1, \dots, m, d_i = \delta$ and for $i = m + 1, \dots, N, \lambda_i = 0$. By using the first condition, for $i = 1, \dots, m$, we have $-1 + 2\nu(\delta - a) + \lambda_i = 0$ and for $i = m + 1, \dots, N$, we have $-1 + 2\nu(d_i - a) = 0$. Therefore we have optimal d_i as follow:

$$d_i = \begin{cases} \delta, & i = 1, \dots, m \\ \frac{1}{2\nu} + a, & i = m + 1, \dots, N. \end{cases}$$

Note that if $m = 0$ then this corresponds to the Hyper-Fractionated schedule (all doses equal), and if $m = N - 1$ this is the Semi-Hypo-Fractionated schedule (all doses but one equal to minimum value of δ).

From the third condition, we have

$$d_{m+1} = \dots = d_N = \sqrt{\frac{C - m(\delta - a)^2}{N - m}} + a$$

Using the previous two displays, we can get

$$\sum_{i=1}^N d_i = m\delta + a(N - m) + \sqrt{(N - m)[C - m(\delta - a)^2]}$$

Since $\frac{\partial}{\partial m} \sum_{i=1}^N d_i$ is always negative for all δ , then smaller m results in bigger values of $\sum_{i=1}^N d_i$. Therefore $m = 0$ maximizes $\sum_{i=1}^N d_i$. If we repeat these steps for the minimization problem we will get the second statement of the lemma (in particular we get that $m = N - 1$). □

The previous lemma shows how the maximizer or minimizer of $\sum_{i=1}^N d_i$ on the surface of a N dimensional hypersphere can be located. Therefore when the hyperspheres HSE and HSL do not intersect we can easily find the optimal solutions based on the relative magnitude of the ratios of the $\frac{\alpha}{\beta}$ for the tumor and sensitive tissues using Lemma 1.

We now consider the setting where the hyperspheres HSE and HSL intersect on the feasible region, i.e. when all coordinates are greater than δ . Note that if the hyperspheres intersect on this region then one of them will be closer to the origin along the hyperfractionation plane, i.e. the plane $d_1 = \dots = d_N$, we will denote this as HS1 from this point forward. The remaining hypersphere will be denoted by HS2. We identify HS1 with either HSE or HSL by setting

$$I = \arg \min \left\{ \sqrt{\frac{1}{N} \frac{\alpha_e C_e}{\beta_e \delta_e^2} + \frac{1}{4} \frac{\alpha_e^2}{\beta_e^2 \delta_e^2}} - \frac{1}{2} \frac{\alpha_e}{\beta_e \delta_e}, \sqrt{\frac{1}{N} \frac{\alpha_l C_l}{\beta_l \delta_l^2} + \frac{1}{4} \frac{\alpha_l^2}{\beta_l^2 \delta_l^2}} - \frac{1}{2} \frac{\alpha_l}{\beta_l \delta_l} \right\}, \tag{12}$$

if $I = 1$ then HS1 = HSE; otherwise HS1= HSL. We will now study the extrema of $\sum_{i=1}^N d_i$ on the intersection of HS1 and HS2.

Lemma 2 *The minimum (maximum) value of $\sum_{i=1}^N d_i$ when HS1 (HS2) is the most restrictive constraint occur at the intersection of HS1 and HS2.*

Proof First we find the separating hyperplane of the two hyperspheres at their intersection. Assume the two hyperspheres have the following equations:

$$\begin{aligned} \sum_{i=1}^N (d_i - a_1)^2 &= C_1 \\ \sum_{i=1}^N (d_i - a_2)^2 &= C_2 \end{aligned}$$

For every point (d_1, \dots, d_N) that lies on the intersection of two hyperspheres, the following two equations are satisfied:

$$\sum_{i=1}^N d_i^2 - 2a_1 \sum_{i=1}^N d_i + Na_1^2 = C_1$$

$$\sum_{i=1}^N d_i^2 - 2a_2 \sum_{i=1}^N d_i + Na_2^2 = C_2$$

Hence by subtracting above equations, we can get:

$$\sum_{i=1}^N d_i = \frac{C_1 - Na_1^2 - C_2 + Na_2^2}{2(a_2 - a_1)}$$

Therefore the intersection of two hyperspheres can be described by a separating hyperplane having above equation. The regions where the first and second hypersphere are the most restrictive constraints can be viewed as

$$A_1 = \left\{ (d_1, \dots, d_N) : \sum_{i=1}^N d_i \geq \frac{C_1 - Na_1^2 - C_2 + Na_2^2}{2(a_2 - a_1)} ; \sum_{i=1}^N (d_i - a_1)^2 = C_1 \right\}$$

$$A_2 = \left\{ (d_1, \dots, d_N) \left| \sum_{i=1}^N d_i \leq \frac{C_1 - Na_1^2 - C_2 + Na_2^2}{2(a_2 - a_1)} ; \sum_{i=1}^N (d_i - a_2)^2 = C_2 \right. \right\}$$

The minimization of $\sum_{i=1}^N d_i$ on A_1 is given by the following:

$$\text{Minimize } \sum_{i=1}^N d_i$$

subject to

$$\sum_{i=1}^N (d_i - a_1)^2 = C_1$$

$$\sum_{i=1}^N d_i \geq \frac{C_1 - Na_1^2 - C_2 + Na_2^2}{2(a_2 - a_1)}$$

Obviously the minimum value of the objective function in the previous display occurs when $\sum_{i=1}^N d_i = \frac{C_1 - Na_1^2 - C_2 + Na_2^2}{2(a_2 - a_1)}$.

The maximization of $\sum_{i=1}^N d_i$ when HS2 is the most restrictive constraint can be formulated as:

$$\text{Maximize } \sum_{i=1}^N d_i$$

subject to

$$\sum_{i=1}^N (d_i - a_2)^2 = C_2$$

$$\sum_{i=1}^N d_i \leq \frac{C_1 - Na_1^2 - C_2 + Na_2^2}{2(a_2 - a_1)}$$

The equation $\sum_{i=1}^N d_i = \frac{C_1 - Na_1^2 - C_2 + Na_2^2}{2(a_2 - a_1)}$ satisfies the first constraint and also defines the upper bound of objective function, therefore it is the optimal solution to the maximization problem. \square

In Lemma 1, the problem of optimal fractionation was considered with only a single normal tissue constraint. In the previous lemma, we studied optimizing the total radiation delivered when considering two overlapping normal tissue constraints. In the next result we use these two lemmas to solve the optimal fractionation problem posed in (8).

Before stating the result we need further notation. In particular, if the two hyperspheres HSE and HSL do not intersect then denote the parameters of the more restrictive hypersphere by $\alpha_x, \beta_x,$ and δ_x . If the hyperspheres intersect then denote the parameters corresponding to HS1 [as identified in (12)] by $\alpha_1, \beta_1,$ and δ_1 ; similarly denote the parameters corresponding to HS2 by $\alpha_2, \beta_2,$ and δ_2

Theorem 2 *There are three different solutions for (8). The solutions may be grouped into the three following classes:*

- I. *If $\alpha - \frac{\beta\alpha_1}{\beta_1\delta_1}$ and $\alpha - \frac{\beta\alpha_e}{\beta_e\delta_e}$ are both positive; or HSE and HSL don't intersect and $\alpha - \frac{\beta\alpha_x}{\beta_x\delta_x}$ is positive, then the optimal dose vector is a hyperfractionated schedule with all doses equal to*

$$d^* = \min \left\{ \sqrt{\frac{1}{N} \frac{\alpha_e C_e}{\beta_e \delta_e^2} + \frac{1}{4} \frac{\alpha_e^2}{\beta_e^2 \delta_e^2}} - \frac{1}{2} \frac{\alpha_e}{\beta_e \delta_e}, \sqrt{\frac{1}{N} \frac{\alpha_l C_l}{\beta_l \delta_l^2} + \frac{1}{4} \frac{\alpha_l^2}{\beta_l^2 \delta_l^2}} - \frac{1}{2} \frac{\alpha_l}{\beta_l \delta_l} \right\}. \tag{13}$$

- II. *If both $\alpha - \frac{\beta\alpha_1}{\beta_1\delta_1}$ and $\alpha - \frac{\beta\alpha_e}{\beta_e\delta_e}$ are negative; or HSE and HSL don't intersect and $\alpha - \frac{\beta\alpha_x}{\beta_x\delta_x}$ is negative then the optimal dose vector is a semi-hypofractionated schedule where*

$$d_i = \min \left\{ \sqrt{\frac{\alpha_e C_e}{\beta_e \delta_e^2} + N \left(\frac{1}{2} \frac{\alpha_e}{\beta_e \delta_e} \right)^2} - (N - 1) \left(\delta + \frac{1}{2} \frac{\alpha_e}{\beta_e \delta_e} \right)^2 \right. \\ \left. - \frac{1}{2} \frac{\alpha_e}{\beta_e \delta_e}, \sqrt{\frac{\alpha_l C_l}{\beta_l \delta_l^2} + N \left(\frac{1}{2} \frac{\alpha_l}{\beta_l \delta_l} \right)^2} - (N - 1) \left(\delta + \frac{1}{2} \frac{\alpha_l}{\beta_l \delta_l} \right)^2 - \frac{1}{2} \frac{\alpha_l}{\beta_l \delta_l} \right\}$$

$$d_j = \delta \quad \forall j = 1, \dots, N (j \neq i). \tag{14}$$

III. If HSE and HSL intersect, $\alpha - \frac{\beta\alpha_1}{\beta_1\delta_1}$ is negative and $\alpha - \frac{\beta\alpha_2}{\beta_2\delta_2}$ is positive the solution vector lies on the surface of the two hyperspheres:

$$\sum_{i=1}^N \left(d_i + \frac{1}{2} \frac{\alpha_e}{\beta_e \delta_e} \right)^2 = \frac{\alpha_e C_e}{\beta_e \delta_e^2} + N \left(\frac{1}{2} \frac{\alpha_e}{\beta_e \delta_e} \right)^2 \tag{15}$$

$$\sum_{i=1}^N \left(d_i + \frac{1}{2} \frac{\alpha_l}{\beta_l \delta_l} \right)^2 = \frac{\alpha_l C_l}{\beta_l \delta_l^2} + N \left(\frac{1}{2} \frac{\alpha_l}{\beta_l \delta_l} \right)^2 \tag{16}$$

Proof First we analyze the case that HSE and HSL do not intersect. In this case, one of them is redundant and we need only consider the most restrictive hypersphere. For two-dimensional case, this problem is described in Fig. 2. In Fig. 2a, the ratio of $\frac{\beta\alpha_l}{\beta_l\delta_l}$ or $\frac{\beta\alpha_e}{\beta_e\delta_e}$ related to the smaller circle determines the optimal schedule regime and in Fig. 2b, the optimal doses can be found with respect to the ratio of $\frac{\beta\alpha_l}{\beta_l\delta_l}$ or $\frac{\beta\alpha_e}{\beta_e\delta_e}$ related to the bigger circle. According to Lemma 1, $\sum_{i=1}^N d_i$ is maximized when $d_1 = \dots = d_N$ (Hyper-Fractionated) and is minimized when one of the d_i is big and others take δ (Semi-Hypo-Fractionated). Optimal doses can be calculated by the maximum amount of BED that late and early tissues can bear. From Lemma 1 and the discussion after (11), the optimal doses when $\alpha - \frac{\beta\alpha_x}{\beta_x\delta_x} \geq 0$ are given by the hyper-fractionated schedule with all $d_i = d^*$ and

$$d^* = \min \left\{ \sqrt{\frac{1}{N} \frac{\alpha_e C_e}{\beta_e \delta_e^2} + \frac{1}{4} \frac{\alpha_e^2}{\beta_e^2 \delta_e^2}} - \frac{1}{2} \frac{\alpha_e}{\beta_e \delta_e}, \sqrt{\frac{1}{N} \frac{\alpha_l C_l}{\beta_l \delta_l^2} + \frac{1}{4} \frac{\alpha_l^2}{\beta_l^2 \delta_l^2}} - \frac{1}{2} \frac{\alpha_l}{\beta_l \delta_l} \right\}.$$

When $\alpha - \frac{\beta\alpha_x}{\beta_x\delta_x} < 0$ the optimal solution are given by the Semi-Hypo-Fractionated schedules

$$d_i = \min \left\{ \sqrt{\frac{\alpha_e C_e}{\beta_e \delta_e^2} + N \left(\frac{1}{2} \frac{\alpha_e}{\beta_e \delta_e} \right)^2} - (N - 1) \left(\delta + \frac{1}{2} \frac{\alpha_e}{\beta_e \delta_e} \right)^2, \right. \\ \left. - \frac{1}{2} \frac{\alpha_e}{\beta_e \delta_e}, \sqrt{\frac{\alpha_l C_l}{\beta_l \delta_l^2} + N \left(\frac{1}{2} \frac{\alpha_l}{\beta_l \delta_l} \right)^2} - (N - 1) \left(\delta + \frac{1}{2} \frac{\alpha_l}{\beta_l \delta_l} \right)^2 - \frac{1}{2} \frac{\alpha_l}{\beta_l \delta_l} \right\}$$

$$d_j = \delta \quad \forall j = 1, \dots, N (j \neq i)$$

In the case that HSE and HSL intersect, we face four different situations:

1. $\alpha - \frac{\beta\alpha_1}{\beta_1\delta_1} \geq 0$ and $\alpha - \frac{\beta\alpha_2}{\beta_2\delta_2} \geq 0$: In this case, we want to maximize $\sum_{i=1}^N d_i$ on both hyperspheres. According to Lemma 1, the maximum value of $\sum_{i=1}^N d_i$ on the surface of a hypersphere is given by a Hyper-Fractionated schedule. Based on our assumption, Hyper-Fractionated schedule is only feasible on HS1. In Lemma 2, we showed that the minimum (maximum) of $\sum_{i=1}^N d_i$ on the boundaries of HS1 (HS2), occurs at the intersection of two hyperspheres. Therefore d_1, \dots, d_N obtained by

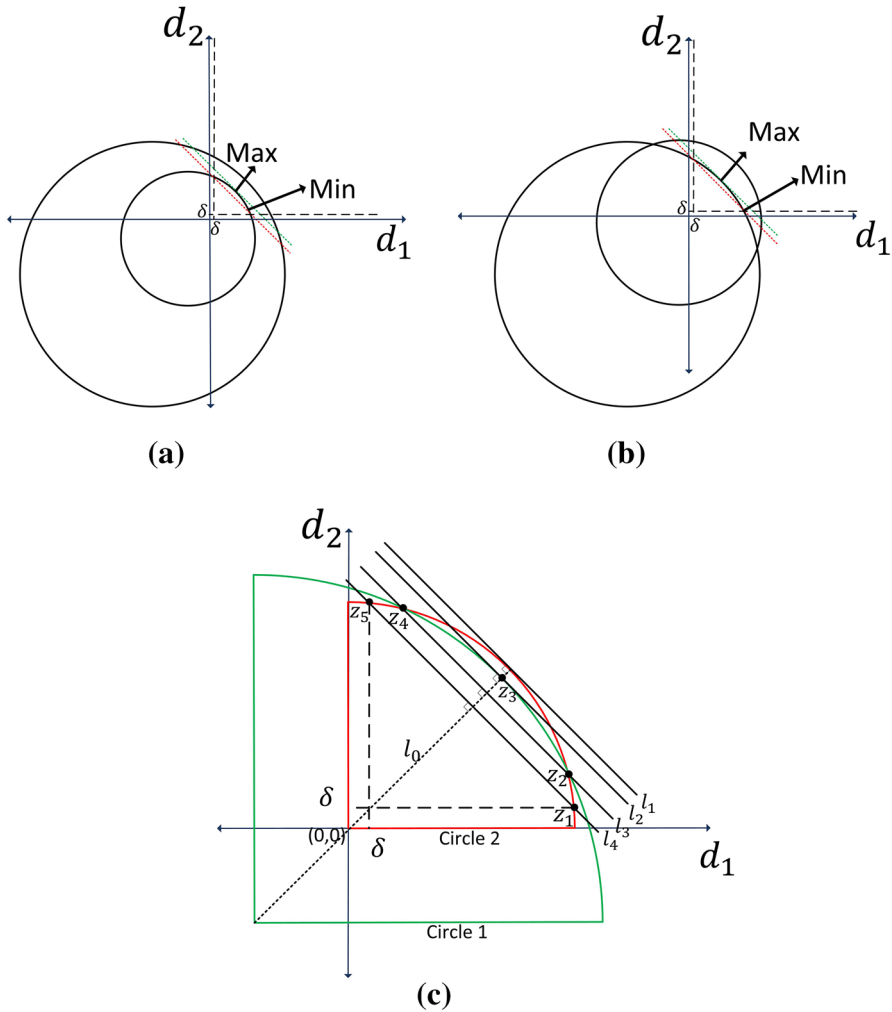


Fig. 2 **a, b** Maximum and minimum conditions of $d_1 + d_2$ under the constraint for the radiation effect on tumor (two hyperspheres don't intersect). The ratio of $\frac{\beta\alpha_1}{\beta_1\delta_1}$ or $\frac{\beta\alpha_e}{\beta_e\delta_e}$ related to the smaller circle determines the optimal schedule regime in **a** and the optimal doses (d_1 and d_2) can be found with respect to the ratio of $\frac{\beta\alpha_1}{\beta_1\delta_1}$ or $\frac{\beta\alpha_e}{\beta_e\delta_e}$ related to the bigger circle in **b**. **c** Feasible region for two-dimensional case (two hyperspheres intersect). The feasible boundaries are arcs between points Z_1, Z_2, Z_3, Z_4 and Z_5 . The maximum (minimum) value of $d_1 + d_2$ on both quadrants happens at Z_3 (Z_1 and Z_5). Also the maximum (minimum) value of $d_1 + d_2$ on the red (green) quadrant and the minimum (maximum) value of $d_1 + d_2$ on the green (red) quadrant happen at Z_2 and Z_4 (either Z_3 or Z_1 and Z_5) (color figure online)

Hyper-Fractionated schedule on hypersphere 1 have the biggest value of $\sum_{i=1}^N d_i$ among all feasible points. Thus the optimal schedule is Hyper-Fractionated schedule with equal doses obtained from (13). For 2-dimensional case, the feasible boundaries in the Fig. 2c are arcs between points Z_1, Z_2, Z_3, Z_4 and Z_5 . We draw

4 contours of the function $d_1 + d_2 = c$ for different c in Fig. 2c (contours are illustrated by l_1, l_2, l_3 and l_4 which except l_1 , others touch feasible region). In Fig. 2c, a point with the largest distance from origin is Z_3 .

2. $\alpha - \frac{\beta\alpha_1}{\beta_1\delta_1} < 0$ and $\alpha - \frac{\beta\alpha_2}{\beta_2\delta_2} < 0$: In this case, the optimal schedule is a schedule minimizing $\sum_{i=1}^N d_i$ on both hyperspheres. According to Lemma 1, minimum value of $\sum_{i=1}^N d_i$ on the surface of the hypersphere restricted to all coordinates being greater than δ is obtained by a Semi-Hypo-Fractionated schedule. By definition the Semi-Hypo-Fractionated schedule is only feasible on HS2. Based on Lemma 2, we know that the intersection has the lowest (highest) value of objective function on the boundaries of HS1 (HS2), therefore the optimal schedule is located on the boundaries of HS2 and is given by the Semi-Hypo-Fractionated schedule (14). For two-dimensional case, the optimal solution is the contour with the smallest distance from origin on l_0 crossing feasible region. By looking at Fig. 2c, points having this feature can be either Z_1 or Z_5 .
3. $\alpha - \frac{\beta\alpha_1}{\beta_1\delta_1} \leq 0$ and $\alpha - \frac{\beta\alpha_2}{\beta_2\delta_2} > 0$: In this case, we are looking for the minimum value of $\sum_{i=1}^N d_i$ on the boundary of HS1 and its maximum on the boundary of HS2. From Lemma 1 and scenarios 1 and 2 above, we know that schedules having this property lie at the intersection of HS1 and HS2. Therefore we can reach optimal schedule which is represented by a $N - 1$ dimensional hypersphere satisfying (15) and (16). For two dimensional case, the feasible region of circle 1 are two arcs which connect Z_1 to Z_2 and Z_4 to Z_5 . Also the feasible region of circle 2 is the arc which connects Z_2 to Z_4 . If we move from Z_1 (Z_5) toward Z_2 (Z_4), $d_1 + d_2$ increases and if we move from Z_3 toward Z_2 or Z_4 , $d_1 + d_2$ decreases. So the optimal point on both circles are Z_2 and Z_4 which maximize $d_1 + d_2$ on the feasible region of circle 1 and minimize $d_1 + d_2$ on the feasible region of circle 2.

Note that the situation where HSE and HSL intersect, $\alpha - \frac{\beta\alpha_1}{\beta_1\delta_1}$ is positive and $\alpha - \frac{\beta\alpha_2}{\beta_2\delta_2}$ is negative cannot happen, because requiring $\frac{\alpha_1}{\delta_1\beta_1} < \frac{\alpha}{\beta} < \frac{\alpha_2}{\delta_2\beta_2}$ and the definition of HS1 (and HS2) in (12) leads to a contradiction of the intersection HSE and HSL where $d_i \geq \delta \geq 0$. □

In setting (4) we are not able to exactly specify the optimal dose allocation, but instead specify that the dose allocation vector lies on the intersection of two hypersphere surfaces. However, it should be noted that any vector (d_1, \dots, d_N) satisfying (15) and (16) will necessarily have both $\sum_{i=1}^N d_i$ and $\sum_{i=1}^N d_i^2$ fixed. In particular, the effect of any dose allocation vector satisfying (15) and (16) on either normal or tumor tissue is fixed.

3.3.2 Model II

In the second model, we only optimize inter-fraction intervals while assuming that the optimal number of fractions is N . This model can be defined as:

$$\begin{aligned}
 & \text{Minimize}_{t_i} \ln \{ (Rc_4 + c_5)(1 + R) + [-R(c_5 + Rc_4 - c_2) \\
 & + (c_6 - Rc_2 + Rc_3)\gamma_0 e^{-(t_{N-1}-\mu)^2/\sigma^2}] \left[(1 - \gamma_0) \prod_{i=1}^{N-2} (1 - \gamma_0 e^{-(t_i-\mu)^2/\sigma^2}) \right] \} \\
 & \hspace{25em} (17)
 \end{aligned}$$

Subject to:

$$\begin{aligned}
 & \sum_{i=1}^{N-1} t_i = T_p \\
 & t_i \geq \epsilon \quad \forall i.
 \end{aligned}$$

For ease of notation we define the terms $A = -R(c_5 + Rc_4 - c_2)$ and $B = (c_6 - Rc_2 + Rc_3)\gamma_0$.

Theorem 3 *If $\sigma < 2$ time units, $A > 0$, and there exists $k \geq 5$ such that*

$$N_{max}(\mu + \sigma\sqrt{k}) < T_p \tag{A}$$

$$4e^{-k} < \gamma_0 \tag{A1}$$

then the optimal inter-fraction times are of the form $t_i \in [\mu, \mu + \sigma e^{-k/2}]$ for $i \leq N - 2$, and $t_{N-1} = T_p - (t_1 + \dots + t_{N-2})$.

Proof Instead of optimizing the logarithm of (17), we can minimize the term inside the logarithm. By replacing the value of c_i with their definitions in (5), it can be seen that $B = -\gamma_0 A$ and therefore the objective function can be simplified by ignoring the terms A , $(Rc_4 + c_5)(1 + R)$ and $(1 - \gamma_0)$, since they are positive constants. Again we optimize the logarithm of the objective function and observe:

$$\text{Minimize}_{t_i} \sum_{i=1}^{N-1} \ln(1 - \gamma_0 e^{-(t_i-\mu)^2/\sigma^2})$$

Subject to:

$$\begin{aligned}
 & \sum_{i=1}^{N-1} t_i = T_p \\
 & t_i \geq \epsilon, \quad \forall i
 \end{aligned}$$

Since the feasible region for the above optimization problem is compact and the objective function is continuous on it, the problem admits at least one optimum. It is evident that our mathematical model is not convex, so that we can only use the

optimality necessary conditions provided by the Karush Kuhn Tucker (KKT) (Pierre 1969). The first step is constructing the Lagrangian function. Thus for the vector of inter-fraction times $\mathbf{t} = (t_1, \dots, t_{N-1})$:

$$L(\mathbf{t}, \nu, \lambda) = \sum_{i=1}^{N-1} \ln \left(1 - \gamma_0 e^{-(t_i - \mu)^2 / \sigma^2} \right) + \nu \left(\sum_{i=1}^{N-1} t_i - T_p \right) + \sum_{i=1}^{N-1} \lambda_i (t_i - \epsilon) \tag{18}$$

We thus have the KKT conditions:

$$\frac{\partial L}{\partial t_i} = \frac{2\gamma_0(t_i - \mu)}{\sigma^2(e^{(t_i - \mu)^2 / \sigma^2} - \gamma_0)} + \nu + \lambda_i = 0; \quad \forall i \tag{19}$$

$$\sum_{i=1}^{N-1} t_i - T_p = 0 \tag{20}$$

$$\lambda_i \times (t_i - \epsilon) = 0, \quad \forall i \tag{21}$$

$$t_i \geq \epsilon, \quad \lambda_i \leq 0, \quad \nu : \text{free} \tag{22}$$

From (21), it is obvious that one of the conditions $t_i = \epsilon$ or $\lambda_i = 0$ must hold for each i , and further that only one of these conditions may hold at a time. Consider two disjoint sets S_1 and S_2 such that for $i \in S_1$, $t_i = \epsilon$, for $i \in S_2$, $\lambda_i = 0$, and $S_1 \cup S_2 = \{1, \dots, N - 2\}$.

Assume that $S_1 \neq \emptyset$, and observe that for $i \in S_1$, we have the following KKT condition:

$$\frac{\partial L}{\partial t_i} = \frac{2\gamma_0(\epsilon - \mu)}{\sigma^2(e^{(\epsilon - \mu)^2 / \sigma^2} - \gamma_0)} + \nu + \lambda_i = 0. \tag{23}$$

Since $\epsilon < \mu$, $0 \leq \gamma_0 \leq 1$ and $\lambda_i \leq 0$, then $\nu > 0$; thus if $S_1 \neq \emptyset$, we have $\nu > 0$. Also for every $i \in S_2$, we have:

$$\frac{\partial L}{\partial t_i} = \frac{2\gamma_0(t_i - \mu)}{\sigma^2(e^{(t_i - \mu)^2 / \sigma^2} - \gamma_0)} + \nu = 0. \tag{24}$$

Thus from (24), we see $t_i < \mu$ for every $i \in S_2$. Since we impose the condition $N \leq N_{max}$, and assumption (A) we see that if $S_1 \neq \emptyset$ then we cannot satisfy condition (20). Therefore we will always have $\nu \leq 0$, $S_1 = \emptyset$ and $\lambda_i = 0$. Note that if $\nu \leq 0$, then necessarily the optimal $t_i \geq \mu$.

Next define the function

$$h(t) = \frac{2\gamma_0(t - \mu)}{\sigma^2(e^{(t - \mu)^2 / \sigma^2} - \gamma_0)}. \tag{25}$$

From straightforward calculations we observe that $h'(t) < 0$ for $t \geq \mu + \sigma/\sqrt{2}$. For k from condition (A) define $v_k = h(\mu + \sigma\sqrt{k})$, and observe that

$$v_k = \max_{t \geq \mu + \sigma\sqrt{k}} h(t).$$

The previous display implies that if we choose v such that $-v \geq v_k$ then in order to satisfy Eq. (24) it is necessary that $t_i \leq \mu + \sigma\sqrt{k}$ for all i . However condition (A) will then imply it is impossible to satisfy condition (20). We thus conclude that $v \in [-v_k, 0]$.

It now follows that the optimal times necessarily belong to the set

$$\{\mu \leq t \leq T_p : h(t) \in [0, v_k]\} \subset [\mu, \mu + \varepsilon(k)] \cup [\mu + \sigma\sqrt{k}, T_p],$$

where $\varepsilon(k) = \inf\{t \geq \mu : h(t) = v_k\}$. Note that since we require $k \geq 5$ we have that $\varepsilon(k) \leq e^{-k/2}\sigma$. Define the set of indices with large inter-fraction times as

$$J = \{j : t_j \in [\mu + \sigma\sqrt{k}, T_p]\}.$$

In order to establish the result it remains to show that for any optimal set of inter-fraction times $|J| = 1$. Thus consider a set of inter-fraction times $\mathbf{t} = (t_1, \dots, t_{N-1})$ such that $t_1 + \dots + t_{N-1} = T_p$ and $|J| \geq 2$. Define

$$t_m = \min\{t_j; j \in J\}$$

$$t_M = \max\{t_j; j \in J\}.$$

Then consider the new set of feasible inter-fraction times $\mathbf{t}' = (t'_1, \dots, t'_{N-1})$, where $t'_m = \mu$ and $t'_M = t_M + (t_m - \mu)$. We will now establish that

$$L(\mathbf{t}', v, \lambda) \leq L(\mathbf{t}, v, \lambda). \tag{26}$$

Define

$$\ell(t) = \log\left(1 - \gamma_0 e^{-(t-\mu)^2/\sigma^2}\right),$$

then in order to establish (26) it suffices to show

$$\begin{aligned} &\ell(t_m) + \ell(t_M) - \ell(t'_m) - \ell(t'_M) \\ &= \log\left(\frac{\left(1 - \gamma_0 e^{-(t_m-\mu)^2/\sigma^2}\right)\left(1 - \gamma_0 e^{-(t_M-\mu)^2/\sigma^2}\right)}{(1 - \gamma_0)\left(1 - \gamma_0 e^{-(t'_M-\mu)^2/\sigma^2}\right)}\right) > 0, \end{aligned}$$

or equivalently

$$\left(1 - \gamma_0 e^{-(t_m-\mu)^2/\sigma^2}\right)\left(1 - \gamma_0 e^{-(t_M-\mu)^2/\sigma^2}\right) > (1 - \gamma_0)\left(1 - \gamma_0 e^{-(t'_M-\mu)^2/\sigma^2}\right).$$

To establish the previous display it suffices to show that

$$\gamma_0 > \gamma_0 e^{-(t'_M - \mu)^2 / \sigma^2} + e^{-(t_m - \mu)^2 / \sigma^2} + e^{-(t_M - \mu)^2 / \sigma^2},$$

which is of course implied by

$$e^{-(t_m - \mu)^2 / \sigma^2} + e^{-(t_M - \mu)^2 / \sigma^2} < \gamma_0 \left(1 - e^{-(t'_M - \mu)^2 / \sigma^2}\right). \tag{27}$$

Note that by construction $t_m \geq \mu + \sigma\sqrt{k}$ and $t_M \geq \mu + \sigma\sqrt{k}$, and therefore

$$e^{-(t_m - \mu)^2 / \sigma^2} + e^{-(t_M - \mu)^2 / \sigma^2} \leq 2e^{-k}.$$

We also have that $t'_M = t_M + t_m - \mu \geq \mu + 2\sigma\sqrt{k}$ and therefore $e^{-(t'_M - \mu)^2 / \sigma^2} \leq e^{-2k}$, or in other words

$$1 - e^{-(t'_M - \mu)^2 / \sigma^2} \geq 1 - e^{-2k}.$$

Thus (27) is implied by

$$2e^{-k} \leq \gamma_0(1 - e^{-2k}). \tag{28}$$

The quadratic equation gives that the previous display holds for

$$e^{-k} \leq \frac{\sqrt{1 + \gamma_0^2} - 1}{\gamma_0}.$$

However, we use the inequality

$$\frac{\sqrt{1 + \gamma_0^2} - 1}{\gamma_0} \geq \frac{\gamma_0}{4}$$

to see that (28) is implied by condition (A1). □

It should be noted that for the parameters studied in this work we are able to take $k = 15$. Therefore the interval $[\mu, \mu + \sigma e^{-k/2}]$ in any practical setting can be thought of as simply the point $\{\mu\}$. Thus we will assume in Sect. 4 that the optimal treatments are of the form that $N - 2$ inter-fraction times are of length μ and the remaining length is given by $T_p - (N - 2)\mu$.

In order to prove Theorem 3 we needed to assume $A > 0$. One setting where we would lose that assumption is if $r_s > r_d$, in which case the goal would no longer be to minimize the differentiated cell population but instead to minimize the stem-like cell population. Due to the known association between stem-like cells and treatment resistance it might be the case that when dealing with larger schedules and longer time frames it might be of general interest to minimize the stem-like cell population. In future work we will explore counter parts to Theorem 3 when $A < 0$.

3.4 Optimal number of fractions

As mentioned earlier, there are three types of decision variables in this problem (N , $\{d_i\}$ and $\{t_i\}$). By fixing N we were able to locate optimal values of $\{d_i\}$ and $\{t_i\}$ using methods of non-linear programming. In order to find the optimal value of N , we implemented the following algorithm.

Inputs:

- N_{max} : The maximum number of radiation fractions.

Output:

- N^* : The optimal number of radiation fractions.
- t_i^* : The optimal intermediate times between radiation fractions.
- d_i^* : The optimal radiation doses.

Steps:

1. Put $N^* = 1$, and set global objective function as ∞ .
2. Calculate the optimal t_i^* , $i = 1, \dots, N^* - 1$ using the approach presented in 3.3.2.
3. Find the optimal doses for N^* using methodology presented in Sect. 3.3.1.
4. Calculate objective function using t_i^* and d_i^* in (5). If it improves the objective function, save it as the new global optimal solution. Otherwise if $N^* < N_{max}$ set $N^* = N^* + 1$ and go to step 2, otherwise return the optimal global d_i^* , t_i^* and N^* .

Since this approach is guaranteed to terminate after N_{max} steps and each step is a direct calculation based on straightforward formulas we see that as long as N_{max} is not too large this is a feasible algorithm. In our examples we consider N_{max} to be at most 21, but it is clear that this algorithm would also remain feasible for the more realistic value of $N_{max} = 75$.

4 Empirical results

4.1 Parameter values

In order to estimate model parameters, the same approach implemented by Leder et al. (2014) is used. Model fit is carried out by minimizing the mean square error (MSE) between the model predictions and the observed values of volumetric time series data presented in the paper by Leder et al. (2014). Since we assume the same level of radio-sensitivity for both stem-like and differentiated cells, ρ is excluded from our parameter set. The minimization is performed under two constraints. First, the stem-like cells divide less frequently than the differentiated cells, and second that the differentiated cells exit quiescence more quickly than stem-like cells. In addition, based on sensitivity analysis performed by Leder et al. (2014), there are several feasible ranges for some of the model parameters. The relevant ranges for these parameters are reported in the Table 2. The Gradient Descent method is utilized to find the optimal values of model parameters presented in Table 2. The remainder of the tumor parameters in Table 3 are

Table 2 The feasible range for several of our model parameters based on the sensitivity analysis performed by Leder et al. (2014)

Parameter	Range	Unit
α	[0.005, 0.22]	1/Gy
β	[0, 0.0025]	1/Gy ²
γ_0	[0.15, 1]	–
r_d	[0.0028, 0.0045]	1/h
r_s	[0, 0.0015]	1/h
a_s	[0, 0.0025]	1/h
T_d	[0, 160]	h
λ_d	[0.023, ∞]	1/Gy
μ	[1.6, 4]	h
σ^2	[0, 2]	h ²

Table 3 Parameters used for finding optimal schedule derived by minimizing the mean square error (MSE) between the model predictions and the observed values of volumetric time series data presented by Leder et al. (2014)

Parameter	Value	Unit	Parameter	Value	Unit
α	0.2	1/Gy	r_s	0.0008	1/h
β	0.0011	1/Gy ²	a_s	0.0019	1/h
γ_0	0.4	–	R	20	–
ρ	1	–	μ	3.25	h
T_d	159.01	h	σ^2	1.46	h ²
λ_d	0.0654	1/h	T_p	120 or 168	h
T_s	477.02	h	T_e	1000	h
λ_s	0.0328	1/h	α_e/β_e	10	Gy
r_d	0.0038	1/h	α_l/β_l	3	Gy

based on the values reported by Leder et al. (2014). It should be noted that quiescence exit for differentiated cells was modeled by a random variable $L_d + X_d$ by Leder et al. (2014) where L_d is a positive constant and X_d is an exponential random variable with mean $1/\lambda_d$ for a positive rate λ_d . In order to allow for a mathematically tractable model we replaced $L_d + X_d$ with the constant value $T_d = L_d + 1/\lambda_d$. An exactly analogous approach is used for the stem-like cell exit time from quiescence.

For normal tissues we set $\alpha = 0.315/\text{Gy}$ for both late-responding and early responding tissues. The α/β ratio is chosen to be 3 and 10 Gys, for the late-responding and early responding normal tissues, respectively (Yang and Xing 2005). We use the BED of the standard scheme (2 Gys/day \times 5) as the maximum limit of BED for early and late responding normal tissues, C_e and C_l , respectively. Moreover we study optimal schedules for different values of δ_e and δ_l . Table 3 summarizes the values of model parameters used in this paper for tumor, early and late responding normal tissues.

We tested our optimization model for schedules with total time of 120h when considering weekends as break and 168h while allowing treatments during weekend.

Table 4 Optimal dose per fraction for different δ_e and δ_l ($d_1^* = d_2^* = \dots = d_N^*$)

Number of fractions	$\delta_e = \delta_l$			
	0.25 Gy	0.5 Gy	0.75 Gy	1 Gy
$N_{max} = N^* = 15$	0.6882	0.7083	0.727	0.7446
$N_{max} = N^* = 21$	0.4939	0.5108	0.5268	0.542

The response to a given radiation schedule in the context of our mathematical model is measured by the number of tumor cells present 6 weeks after treatment conclusion as an endpoint (approximate tumor doubling time for standard schedule).

4.2 Determination of optimum dosing schedules

Since in clinical practice, patients may visit the clinic at most three times a day, two values for N_{max} are considered: $N_{max} = 15$ where radiation treatments are not allowed on weekends and $N_{max} = 21$ where radiation treatments are allowed during weekends. We constrained the number of patient weekly visits to the clinic by N_{max} , however when solving model II we allow more than 3 visits per day. In both cases, the optimum number of fractions equals to $N^* = 15$ and $N^* = 21$, respectively. Table 4 displays the optimum dose per fraction (optimum times can be calculated from Theorem 3) for $\delta_e = \delta_l = 0.25, 0.5, 0.75, 1$. As expected, the total dose increases with the number of fractions and the dose proportion received by normal tissues. For the same amount of complications in early responding and less amount of complications in late responding tissues than standard schedule, we can increase the total dose by 3.23–11.69% for $N = 15$ and by 3.72–13.82% for $N = 21$ for low and high value of δ , respectively. The optimal dosing times as determined by Theorem 3 are presented in Fig. 3 for $T_p = 120$ and $T_p = 168$.

Due to clinical restrictions, the optimal schedule provided by Theorem 3 is difficult to implement in practice. For example based on our parameter set, the solution to Model II recommends 14 fractions ($N_{max} = 15$) or 20 fractions ($N_{max} = 21$) of radiation in the first two days of their treatment and receive the last dose of radiation on the last day of treatment. In order to study the impact of working hour constraints on the objective function, we find the near optimal schedules in the case that working hour constraints are imposed on the schedules. Specifically we say that working hour constraints require that radiation can only be delivered hourly between 8 a.m. and 5 p.m. It is not possible to find the exact optimal schedule while not violating clinical operating hour constraints using the approach presented in Sect. 3. In this case, our problem is a non-linear interger-programming problem, and we were not able to find the exact optimal solution. We thus utilized the heuristic method of simulated annealing (SA) to locate near optimal schedules satisfying the working hours constraint. In all examples we use 5 million iterations of the SA algorithm. Figure 3 displays the optimal treatment schedule while complying with clinical operating hour constraints for $\delta_e = \delta_l = 0.25, 0.5, 0.75$ and 1, respectively. These data are obtained with maximum fractional dose constraint

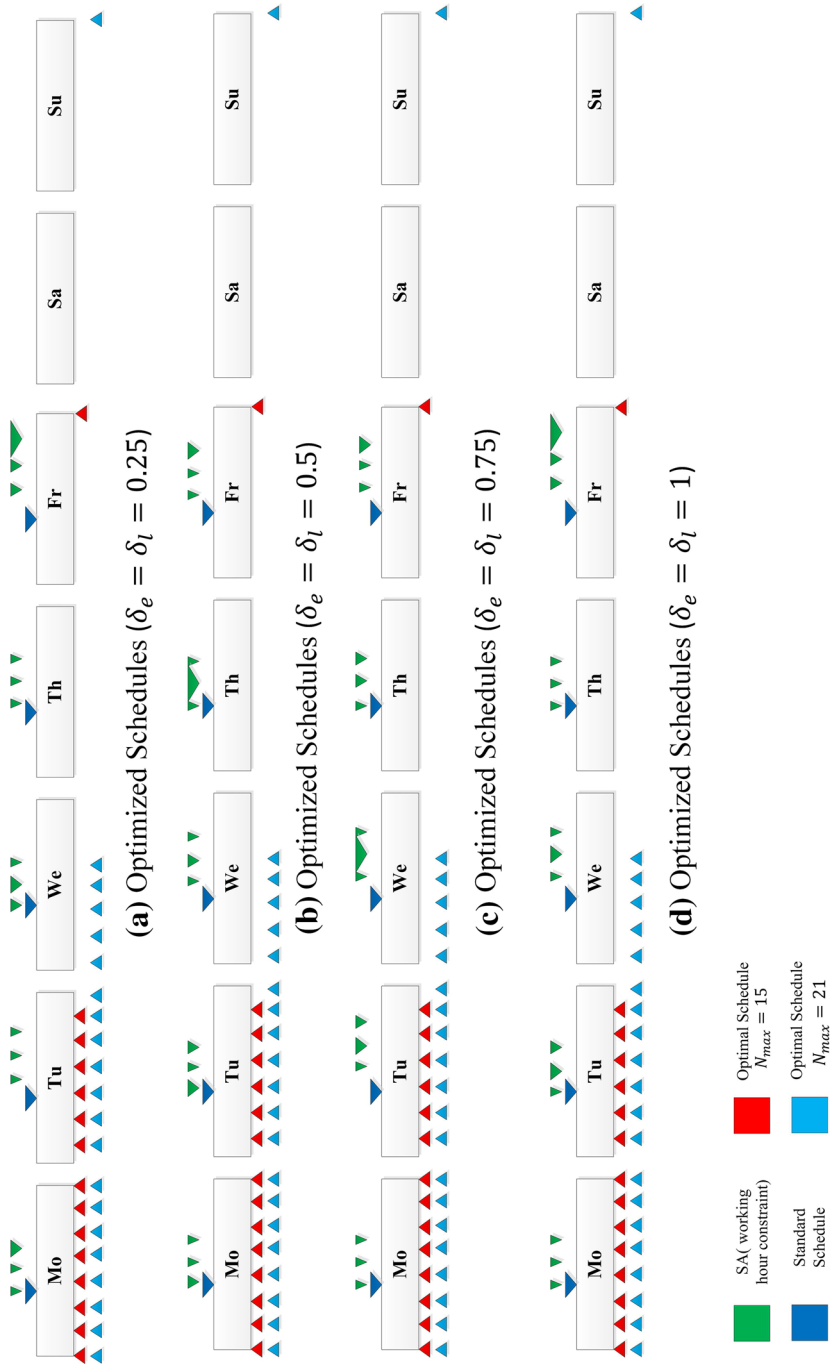


Fig. 3 Schematic depicting the standard, optimum constrained and unconstrained schedules for different δ_e and δ_l . The *arrow position* represents the time of dose during the 1:00 a.m. to 12 p.m. treatment window. The size of the *arrow* correlates with the size of the dose

Table 5 BED of early responding tissues for different schedules

Schedules	δ_e			
	0.25	0.5	0.75	1
Standard schedule	2.625	5.5	8.625	12
Constrained schedule (SA)	2.6242	5.4969	8.618	11.9875
Optimal schedule, $N = 15$	2.625	5.5	8.625	12
Optimal schedule, $N = 21$	2.625	5.5	8.625	12

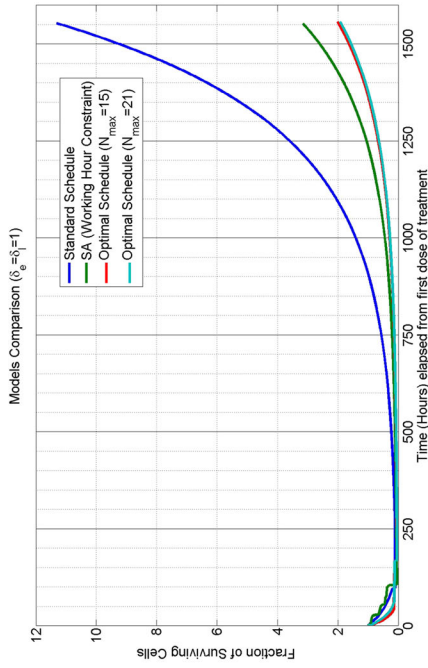
Table 6 BED of late responding tissues for different schedules

Schedules	δ_l			
	0.25	0.5	0.75	1
Standard schedule	2.9167	6.667	11.25	16.6667
Constrained schedule (SA)	2.9141	6.6563	11.2266	16.625
Optimal schedule, $N = 15$	2.7286	5.9389	9.6656	13.9403
Optimal schedule, $N = 21$	2.5997	5.8196	9.3899	13.4397

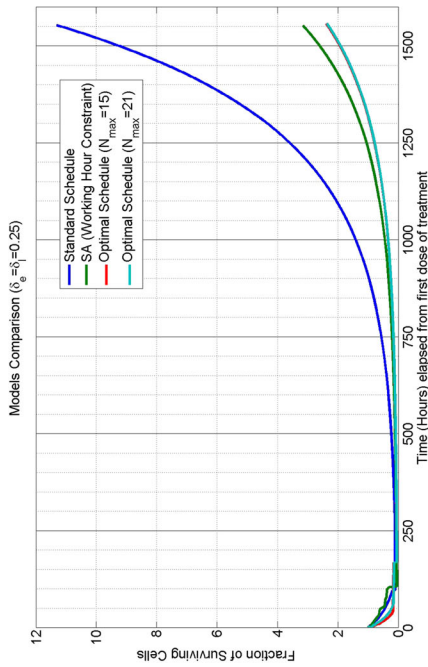
of 5 Gys, administering doses in a multiple of 0.25 Gy of radiation in a single dose and no more than 3 daily visits to the clinic by patient. Furthermore in each iteration, we insure that any schedule created meets the BED constraints for normal tissue. The structure of the optimized therapy focuses most of the radiation on the first and the last slots, has three positive slots per day separated by μ (3 h) and has a large dose of radiation (4 Gys) in an arbitrary slot.

Tables 5 and 6 display BED for early and late responding tissues of different schedules. It is found that the optimized therapy has a BED for late responding tissues that is strictly less than that of the standard and optimized therapy obtained by SA. For the optimal schedules, while delivering more total dose to the tumor, we can reduce BED for late responding tissues for low and high values of δ by 6.5–20%, respectively.

Figure 4 and Table 7 show the predicted tumor growth in response to standard, optimum constrained and unconstrained schedules for different δ_e and δ_l . It is found that the optimum schedules without imposing clinical operating constraint are better than other schedules. The model predicts that optimal unconstrained schedules can increase the tumor doubling time by 400–450 h (37–41%) than standard schedule for low and high values of δ , respectively. Since we can deliver more total dose for high δ_e and δ_l , tumor doubling time increases with the proportionality factor for the normal tissues. The optimum schedule found under working hour constraints is also able to improve predicted survival time. In particular tumor doubling time changes by 325 h (30%) compared to the standard schedule. Note that there is only a loss of roughly 100 h of survival time by imposing working hour constraints.



(a) Model Comparison ($\delta_e = \delta_l = 0.25$)



(b) Model Comparison ($\delta_e = \delta_l = 1$)

Fig. 4 Predicted tumor growth in response to standard, optimum constrained and unconstrained schedules for different δ_e and δ_l

Table 7 Evaluation of radiation damages to the tumor following the treatment and 60 days after treatment beginning

Schedules	$\delta_I = \delta_e = 0.25$		$\delta_I = \delta_e = 0.5$		$\delta_I = \delta_e = 0.75$		$\delta_I = \delta_e = 1$	
	$F_N(0)$ (%)	$F_N(60)$ (%)	$F_N(0)$ (%)	$F_N(60)$ (%)	$F_N(0)$ (%)	$F_N(60)$ (%)	$F_N(0)$ (%)	$F_N(60)$ (%)
Standard schedule	9.48	734.82	9.48	734.82	9.48	734.82	9.48	734.82
Constrained schedule (SA)	4.50	208.06	4.50	208.06	4.50	208.06	4.50	208.06
Optimal schedule, $N = 15$	4.25	156.90	4.00	145.52	3.78	137.52	3.58	130.39
Optimal schedule, $N = 21$	4.21	152.99	3.92	142.45	3.66	133.15	3.44	124.86

Reported values show the fraction of surviving tumor cells following the treatment ($F_N(0)$) and two months after first dose of radiation ($F_N(60)$)

5 Conclusion

In this work, we have analyzed the problem of finding optimum radiation administration schedules for PDGF-driven primary glioblastomas (GBMs). In particular, we aimed to identify the optimized total dose, number of fractions, dose per fraction and inter-fraction intervals for a schedule with a pre-determined fixed treatment duration. We used a simplified version of our previously published model (Leder et al. 2014) to investigate the dynamics of radiation response in two separate populations of cells, stem-like and differentiated cells. We assumed that the dosage delivered to the tumor is constrained by two sensitive structures: the early responding normal tissues that have a relatively high turnover rate, and the late responding tissues that have a slow to undetectable turnover rate.

We have shown that if we fix the number of fractions, our problem can be split into two independent models that can be solved separately. The first model contains only the dose per fraction (which can be used to determine the optimal total dose) as its decision variable. In contrast, the second model only has inter-fraction intervals as its decision variable. For the first model, we proved that any solution must lie on the boundary of the feasible set, i.e., the maximum allowable BED for (at least) one normal tissue complying the second normal tissue constraint. We found that the ratio of the dose that normal tissues absorb and the magnitude of the alpha/beta ratio for both normal tissue and the tumor determine the optimal radiation scheme. Depending on the model parameters, the optimal schedule can be either Hyper-Fractionated or Semi-Hypo-Fractionated (i.e., a fractionation schedule where all doses, but one are equal to minimum value of δ). Note that this solution is valid for the linear-quadratic model with two normal tissue constraints, and is not specific to the de-differentiation model previously developed by Leder et al. (2014).

For the second model, we showed that optimal inter-fraction intervals only depend on the time dynamics of the dedifferentiation process and treatment duration. In particular, in a treatment with N fractions, we found that $N - 2$ inter-fraction intervals are equal to the dose spacing that leads to the maximal amount of cell reversion to the stem-like state (μ), and can be calculated from number of fractions, treatment duration and μ . Lastly, since the total number of fractions is generally limited to be a rather small number, it is then feasible to search through all possible fraction numbers and find the optimal number of fractions.

Using data gathered previously (Leder et al. 2014), we parametrized our model to investigate the behavior of optimal schedules. The theoretical optimum is observed to be a hyper-fractionated schedule with the maximum number of allowable fractions. This optimum is found to increase the model-predicted doubling times from roughly 1000h with standard therapy to roughly 1500h. If we impose realistic operating hours for a radiation clinic (i.e., 8 a.m. to 5 p.m. every day), then the optimization of inter-fraction times becomes too difficult to solve mathematically. We thus utilized the heuristic method of simulated annealing, which is able to find schedules that satisfy working hours constraints and have very good performance. Interestingly we found that for the parameters we considered, there is only a minor cost to adding the working hours constraint. Specifically, Fig. 4 shows that the doubling time for the working

hour constraint problem is roughly 1400h versus the 1500h obtained by ignoring the constraint.

An important extension of this work will be to consider the problem of larger scale schedules, i.e., 60Gy over 6 weeks. A mathematical issue that will make the solution of such problems difficult is that it might not be biologically reasonable to assume that $\rho = 1$ (radio-sensitivity factor for stem-like cells) any longer. In particular, over such long time scales it could be that the stem-like cell population plays a much larger role in tumor repopulation and it is therefore important to incorporate the increased radio-resistance of stem-like cells. If we allow $\rho < 1$ then it appears to us that it will no longer be possible to mathematically optimize this system and it will be necessary to rely purely on heuristic approaches such as simulated annealing. This is currently the subject of ongoing work.

This work considers the problem of finding radiation schedules that optimally delay regrowth of tumor populations. The response to radiation is based on the model developed by Leder et al. (2014). While the parameters for the present work are focused on glioma and a particular mouse models of the PDGF-driven subtype of the disease, our work is applicable to a wider range of cancers that are treated via ionizing radiation. In particular, we are very eager to further investigate additional cancers where we can leverage our ability to split the optimization problem (7) into two tractable optimization problems.

Acknowledgments HB is partially supported by NSF Grants CMMI-1362236. KL is partially supported by NSF Grants DMS-1224362 and CMMI-1362236. FM is partially supported by the Grant NIH U54CA143798. E.H is supported by NIH grants U54 CA143798 and U54CA163167-01. We would like to thank an anonymous referee for their helpful comments.

Appendix

Technical lemma

We prove here a technical lemma, which is quite standard but we provide a proof for completeness.

Lemma 3 For $a > 0$ and f a bounded function on $[0, a]$ and continuous at 0,

$$\lim_{\nu \rightarrow \infty} \nu \int_0^a e^{-\nu y} f(y) dy = f(0).$$

Proof First note that

$$\nu \int_0^a e^{-\nu y} f(y) dy - f(0) = \nu \int_0^a e^{-\nu y} (f(y) - f(0)) dy - f(0)e^{-\nu a},$$

and it thus suffices to establish that

$$\lim_{\nu \rightarrow \infty} \nu \int_0^a e^{-\nu y} (f(y) - f(0)) dy = 0.$$

For $\nu > 0$, define $\ell(\nu) = \log(\nu)/\nu$ and then consider the decomposition

$$\begin{aligned} \nu \int_0^a e^{-\nu y} (f(y) - f(0)) dy &= \nu \int_0^{\ell(\nu)} e^{-\nu y} (f(y) - f(0)) dy \\ &\quad + \nu \int_{\ell(\nu)}^a e^{-\nu y} (f(y) - f(0)) dy \\ &\leq \max_{y \leq \ell(\nu)} |f(y) - f(0)| \nu \int_0^{\ell(\nu)} e^{-\nu y} dy \\ &\quad + 2 \max_{y \leq a} |f(y)| \nu \int_{\ell(\nu)}^a e^{-\nu y} dy \\ &\leq \max_{y \leq \ell(\nu)} |f(y) - f(0)| + 2 \max_{y \leq a} |f(y)| / \nu. \end{aligned}$$

Both terms on the final line in the previous display then go to 0 as $\nu \rightarrow \infty$ due to our assumptions on the function f . \square

References

- Bertuzzi A, Bruni C, Papa F, Sinisgalli C (2013) Optimal solution for a cancer radiotherapy problem. *J Math Biol* 66(1–2):311–349
- Bleau A, Hambardzumyan D, Ozawa T, Fomchenko E, Huse J, Brennan C, Holland E (2009) PTEN/PI3K/Akt pathway regulates the side population phenotype and ABCG2 activity in glioma tumor stem-like cells. *Cell Stem Cell* 4(3):226–235
- Brennan C, Momota H, Hambardzumyan D, Ozawa T, Tandon A, Pedraza A, Holland E (2009) Glioblastoma subclasses can be defined by activity among signal transduction pathways and associated genomic alterations. *PLoS One* 4(11):e7752
- Brenner D, Hlatky L, Hahnfeldt P, Huang Y, Sachs R (1998) The linear-quadratic model and most other common radiobiological models result in similar predictions of time-dose relationships. *Radiat Res* 150(1):83–91
- Brenner D (2008) The linear-quadratic model is an appropriate methodology for determining isoeffective doses at large doses per fraction. *Semin Radiat Oncol* 18:234–239
- Charles N, Ozawa T, Squatrito M, Bleau A, Brennan C, Hambardzumyan D, Holland E (2010) Perivascular nitric oxide activates notch signaling and promotes stem-like character in PDGF-induced glioma cells. *Cell Stem Cell* 6(2):141–152
- Chen J, Li Y, Yu T, McKay R, Burns D, Kernie S, Parada L (2012) A restricted cell population propagates glioblastoma growth after chemotherapy. *Nature* 488(7412):522–526
- Dale R, Jones B (2007) Radiobiological modelling in radiation oncology. Lippincott Williams & Wilkins, Philadelphia
- Dionysiou D, Stamatakos G, Uzunoglu N, Nikita K, Marioli A (2004) A four-dimensional simulation model of tumor response to radiotherapy in vivo: parametric validation considering radiosensitivity, genetic profile and fractionation. *J Theor Biol* 230(1):1–20
- Fowler J (2010) 21 years of effective dose. *Br J Radiol* 83:554–568
- Fowler J (1989) The linear-quadratic formula and progress in fractionated radiotherapy. *Br J Radiol* 62(740):679–694
- Hall E, Giaccia A (2006) Radiobiology for the radiologist. Lippincott Williams & Wilkins, Philadelphia
- Harpold H, Alvord E, Swanson K (2007) The evolution of mathematical modeling of glioma proliferation and invasion. *J Neuropathol Exp Neurol* 66(1):1–9
- Howlader N, Noone AM, Krapcho M, Garshell J, Neyman N, Altekruse SF, Kosary CL, Yu M, Ruhl J, Tatalovich Z, Cho H, Mariotto A, Lewis DR, Chen HS, Feuer EJ, Cronin KA (eds) (2013) SEER cancer statistics review, 1975–2010. National Cancer Institute, Bethesda

- Laperriere N, Zuraw L, Cairncross G, Cancer Care Ontario Practice Guidelines Initiative Neuro-Oncology Disease Site Group (2002) Radiotherapy for newly diagnosed malignant glioma in adults: a systematic review. *Radiother Oncol* 64(3):259–273
- Leder K, Pitter K, LaPlant Q, Hambardzumyan D, Ross B, Chan T, Holland E, Michor F (2014) Mathematical modeling of PDGF-driven glioblastoma reveals optimized radiation dosing schedules. *Cell* 156(3):603–616
- Lu W, Chen M, Chen Q, Ruchala K, Olivera G (2008) Adaptive fractionation therapy: I. Basic concept and strategy. *Phys Med Biol* 53(19):5495
- Mizuta M, Takao S, Date H, Kishimoto N, Sutherland L, Onimaru R, Shirato H (2012) A mathematical study to select fractionation regimen based on physical dose distribution and the linear-quadratic model. *Int J Radiat Oncol Biol Phys* 84(3):829–833
- Orlandi E, Palazzi M, Pignoli E, Fallai C, Giostra A, Olmi P (2010) Radiobiological basis and clinical results of the simultaneous integrated boost (SIB) in intensity modulated radiotherapy (IMRT) for head and neck cancer: a review. *Crit Rev Oncol Hematol* 73(2):111–125
- Pajonk F, Vlashi E, McBride W (2010) Radiation resistance of cancer stem cells: the 4 R's of radiobiology revisited. *Stem Cells* 28(4):639–648
- Phillips H, Kharbanda S, Chen R, Forrest W, Soriano R, Wu T, Misra A, Nigro J, Colman H, Soroceanu L et al (2006) Molecular subclasses of high-grade glioma predict prognosis, delineate a pattern of disease progression, and resemble stages in neurogenesis. *Cancer Cell* 9(3):157–173
- Phillips H, Kharbanda S, Chen R, Forrest W, Soriano R, Wu T, Aldape K (2006) Molecular subclasses of high-grade glioma predict prognosis, delineate a pattern of disease progression, and resemble stages in neurogenesis. *Cancer Cell* 9(3):157–173
- Pierre D (1969) Optimization theory with applications. Wiley, New York
- Rich J (2007) Cancer stem cells in radiation resistance. *Cancer Res* 67(19):8980–8984
- Rockne R, Alvord E, Rockhill J, Swanson K (2009) A mathematical model for brain tumor response to radiation therapy. *J Math Biol* 58(4–5):561–578
- Stamatakos G, Antipas V, Uzunoglu N, Dale R (2006) A four-dimensional computer simulation model of the in vivo response to radiotherapy of glioblastoma multiforme: studies on the effect of clonogenic cell density. *Br J Radiol* 79:389–400
- Unkelbach J, Craft D, Salari E, Ramakrishnan J, Bortfeld T (2013) The dependence of optimal fractionation schemes on the spatial dose distribution. *Phys Med Biol* 58(1):159
- Verhaak R, Hoadley K, Purdom E, Wang V, Qi Y, Wilkerson M, Cancer Genome Atlas Research Network (2010) Integrated genomic analysis identifies clinically relevant subtypes of glioblastoma characterized by abnormalities in PDGFRA, IDH1, EGFR, and NF1. *Cancer Cell* 17(1):98–110
- Withers R (1975) The four R's of radiotherapy. *Adv Radiat Biol* 5(3):241–271
- Yang Y, Xing L (2005) Optimization of radiotherapy dose-time fractionation with consideration of tumor specific biology. *Med Phys* 32(12):3666–3677